Optimizing Fourier Filtering for
Digital Holographic Particle Image Velocimetry

T.A. Ooms[*], W.D. Koek[#], V.S.S. Chan[*], J.J.M. Braat[#] & J. Westerweel[*]

[*] **Laboratory for Aero&Hydrodynamics, Delft University of Technology, The Netherlands**
[#] **Optics Research Group, Delft University of Technology, The Netherlands**

e-mail: t.a.ooms@wbmt.tudelft.nl

Abstract

In digital holography, the optical numerical apperature (NA) is limited by the relatively large pixel size of the CCD camera. This results in a relatively large depth of focus of the system. Additionally, the anisotropic light scattering behavior of the seeding particles tends to further reduce the effective NA. This paper shows numerically and experimentally that this additional reduction of the NA can be suppressed by applying appropriate Fourier filtering. This filtering comes with an acceptable reduction of the hologram exposure.

The measurement setup and the method of numerically reconstructing the images of seeding particles in a volume are described. The light scattering pattern of the seeding particles is measured and its relevance for the design of an optimal Fourier filters is described. Then, the performance of three Fourier filters is analyzed numerically and experimentally. As shown in figure 1, by optimizing Fourier filtering, the depth of focus is improved by a factor 10 without a significant increase in the diffraction limit. Finally, measurements indicate that the holographic setup is able to successfully reconstruct a particle's 3-dimensional position.
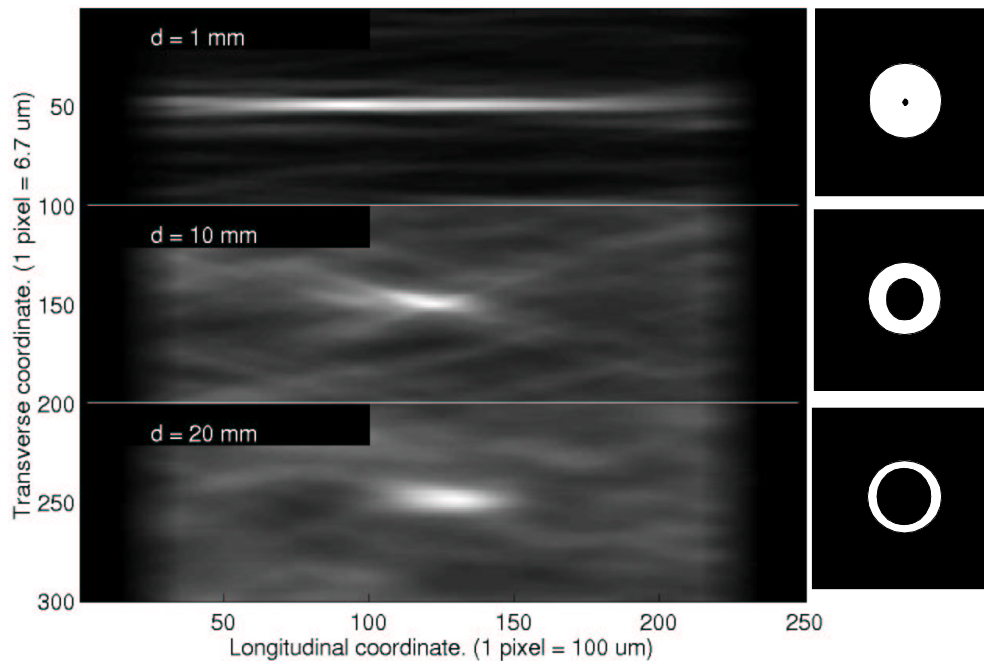
Figure 1. On the left side are slices through three reconstructions of a seeding particle. During the recording of these particles, three different Fourier filters were used, as shown on the right side of the figure. They consist of a concentric opaque disk and a circular aperture. The diameter of the opaque disc is chosen at 1 mm, 10 mm and 20 mm. The diameter of the aperture is constant, 24 mm.

1 Introduction

Digital Holographic Particle Image Velocimetry (DHPIV) is becoming increasingly popular [1-5, 8, 9]. It provides many practical advantages by avoiding the time-consuming steps of Optical Holographic Particle Image Velocimetry (OHPIV). However, as a consequence of the relatively large CCD pixel size (about ten times larger than the typical wavelength of the illumination) the performance of a DHPIV setup is limited. Only a setup with a small optical Numerical Aperture (NA) can lead to successful recordings. An object with a size of a few tens of microns has a theoretical depth of focus of typically more than one millimeter. The accuracy with which a particle's position can be determined along the optical axis is therefore relatively poor. The maximal NA allowed by this restriction is called the *nominal* NA.

Various approaches have focused on improving the low nominal NA. Stereoscopic holography can successfully remove the uncertainty along one axis by viewing from another (perpendicular) direction [1] [2][3][4]. Pan and Meng[5] studied the use of the phase of the reconstructed light wave (only available in digital holography) to increase the accuracy of the reconstructed particle's depth coordinate.

Next to the limiting effect of the CCD chip on the NA, anisotropic forward scattering behavior of the seeding particles tends to further reduce the NA. Most of the scattered light travels in the forward direction in a very narrow cone, as is clearly illustrated in figure 2, [6] and [7]. This effect makes the *effective* NA even smaller than the nominal NA. Although recording 90°-side-scattering would improve isotropy, the extreme reduction of light intensity (figure 2) makes this an unfavorable solution.
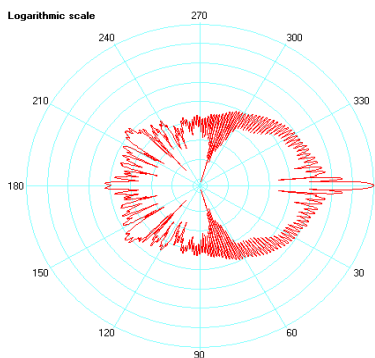

Figure 2. Scattering light intensity as a function of the scattering angle. This figure illustrates that most of the light that scatters from a 20 μm-particle travels in the forward direction. Note that the scale is logarithmic and that forward scattering is about 1000 times stronger than scattering at 20 degrees! (Source: www.philiplaven.com/mieplot.htm)

This paper reports on numerical and experimental results that show how this NA-reducing effect of particle forward-scattering behavior can be suppressed by applying appropriate Fourier filtering. It is shown that the effective NA can be increased towards the nominal NA. This improvement comes with an acceptable reduction of the hologram exposure of a factor 10.

Applying Fourier filtering to an optical (non-digital), off-axis holographic PIV setup to improve the NA has been proposed before [8]. Improvement of the NA was investigated only numerically for a single Fourier filter. This paper, however, focuses on digital holographic PIV and analyzes multiple Fourier filters both numerically and experimentally.

2. Measurement set-up & Data analysis

Our DHPIV setup essentially combines scattered light from seeding particles with a reference beam to form fringes on a CCD camera. The various elements of the setup and the reasons for certain design choices are described in this section. Also, the steps of the digital reconstruction of the hologram are described in this section.

During the description of the measurement setup, the terms 'transverse direction' and 'longitudinal direction' will be used. The first term implies the direction perpendicular to the optical axis, or x- and y-direction. The second term implies the direction along the optical axis, or z-direction.

The illumination is generated by a diode-pumped continuous-wave 150 mW laser (Coherent, Compass 315M-150), and has a wavelength of 532 nm. The laser beam is expanded, collimated and then split into an object beam and a reference beam. The first beam illuminates the object, consisting of several 60 μm-seeding particles. Although the final goal of the system is to perform flow measurements, currently, holograms are recorded of stationary seeding particles. The stationary particles are suspended in a tank filled with resin. This allows for full control of the position of the particles and hence for calibration measurements on the system. The experiment makes use of the forward-scattered light, the so-called in-line set-up.
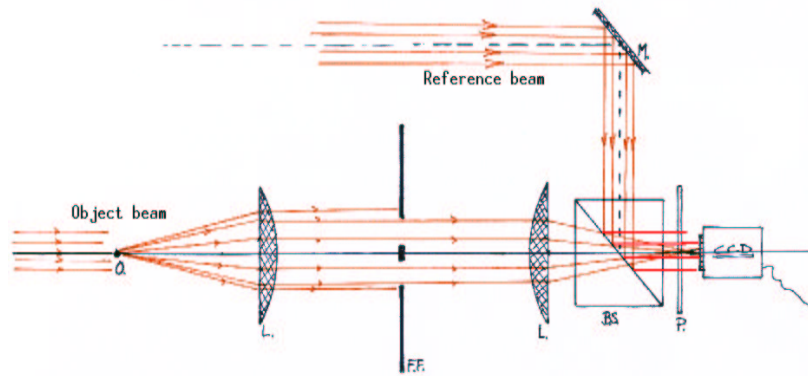

Figure 3. Optical configuration for recording a digital hologram. O is the recorded object. L is a plano-convex lens. FF is an optical Fourier filter. BS is a beam splitter. M is a high-power mirror. P is a linear polarizer and CCD the digital CCD camera.

The scattered light goes through a positive plano-convex lens with a focal length of 300 mm and a diameter of 50 mm, through an optical Fourier filter and through a second identical positive lens. The two lenses are separated by twice their focal distance. The particles near the left focal plane of the left lens have a real image near the right focal plane of the right lens. The coinciding focal plane of both lenses is the Fourier plane. A position in this Fourier plane corresponds to a spatial frequency of the light traveling away from the object plane. Therefore, the intensity pattern as a function of the scattering angle (figure 2) appears in the Fourier plane as a function of a spatial coordinate, x and y. An optical filter can be placed in the Fourier plane to transmit, block or attenuate a certain spatial frequency of the light scattered from the object. A further detailed treatment of Fourier optics is found in Goodman [10]. The choice for the focal length of the lenses is closely related to the combination with the Fourier filter. As shown further in this section, the camera should not register scattered light traveling with an angle of more than 2.3 degrees from the optical axis. Therefore it is desirable that the Fourier filter can transmit (and possibly filter) light traveling with an angle less than 2.3 degrees. Due the cylindrical symmetry, the area on the Fourier filter where filtering should be possible is a circle with radius:

$$R = L_{focal} \cdot \tan(\phi_{cut\text{-}off}) \tag{1}$$

For the given focal length and angle, the radius is 12 mm. A potential way to filter the light may be by passing the light through a suitably exposed negative of a standard 35 mm-film. The dimension of such a negative is 35 x 24 mm. The above described circle with radius 12 mm fits exactly on this negative. Therefore the focal length should not be chosen larger than 300 mm for this setup. Choosing the focal length much smaller could result in an impractically small Fourier filter.

The Fourier filter in this set-up consists of a concentric opaque disc and a larger aperture. Because this setup consists of a separate object beam and reference beam, a Fourier filter is applied to remove the irrelevant, bright, unscattered object beam from the relevant scattered light. In order to realize this, an opaque disc is placed on the optical axis, in the Fourier plane. This disc blocks the unscattered beam if its size is larger than the diffraction limit in the Fourier plane, or 4 µm. Furthermore, an appropriate size of this disc can enhance the effective NA of the system, as is shown in section 4.

As shown further in this section, scattered light that travels with an angle larger than 2.3 degrees from the reference beam (and the optical axis) should not be able to reach the CCD camera. For this reason, an aperture with (an earlier calculated) diameter of 24 mm is placed in the Fourier plane.

The filtered light is combined with the reference beam by a beam splitter and then travels through a linear polarizer. As a result of this measure, all light that reaches the CCD is polarized in the same plane. Light that is scattered from the seeding particles could lose part of its polarization. If the light that reaches the CCD is not polarized in one plane, it would have a negative effect on the contrast of the fringes in the hologram.

The combined beams form a hologram on the CCD chip of a lens-less digital camera (Sensicam 690LL). The CCD chip has 1376 x 1040 pixels with a pixel size of 6.7 µm. The reference beam and the object beam propagate towards the CCD camera along the same axis, the so-called on-axis set-up. According to the Nyquist sampling criterion, the smallest wavelength of the fringe pattern on the CCD camera should be larger than twice the CCD-pixel size, making the maximum angle with which the scattered object light and the reference beam can travel towards the CCD chip,

$$\phi_{max} = \arcsin\left(\frac{\lambda}{(2 \cdot L_{pixel})}\right) \qquad\qquad (2)$$

where λ is the wavelength, 532 nm, and L_{pixel} is the pixel spacing, 6.7 µm. The resulting maximum interference angle is 2.3 degrees. These calculations assume pixels with finite spacing and an infinitely small light-sensitive area, or a zero percent fill-factor. In this theoretical case, aliasing on the CCD chip is avoided by keeping the interference angle smaller than 2.3 degrees. In practice, the fill-factor is finite, and keeping the interference angle roughly below 2.3 degrees is sufficient for an optimal signal-to-noise ratio in the reconstruction.

To make a successful hologram, attention should be paid to the position of the CCD camera. The camera should be positioned about a centimeter in front or behind the real image. If the CCD is closer to the real image, the virtual image in the reconstruction could be about as bright as the real image in the reconstruction, preventing a successfully read out of a particle's position. On the other hand, if the CCD camera is positioned too far from the real image, another problem occurs: The 3-D image of a particle looks like a cone along the optical axis. The narrow point of this cone coincides with the particle position. If the camera is placed to far backward, possibly, only a part of the cross section of the cone falls onto the camera. This will negatively effect the depth of focus, because only the combination of all the light rays of the cone contains accurate information about the particle position. This is illustrated in figure 4.

Then, on a personal computer (CPU: AMD 2.5 GHz; OS: Linux), using Matlab, a reconstruction volume is derived from the digital hologram. The following numerical steps are performed by a simulation: A selection of 1024 x 1024 pixels is taken from the original hologram to improve calculation speed. A kernel, K(x,y), representing the Fresnel approximation of a light wave from a point source, is defined:

$$K(x, y) = \exp\left(\frac{i \cdot k \cdot (x^2 + y^2)}{(2\,z)}\right) \qquad\qquad (3)$$

where i is the imaginary unit, k is the wavenumber of the light, x and y are the transverse coordinates and z is equal to the distance from the CCD chip to a parallel reconstruction plane. The reconstruction image in this plane is obtained from the convolution of the recorded hologram and the above-described kernel. The reconstruction volume is constructed by placing the reconstruction planes in front of each other.

The signal-to-noise ratio of this volume is further improved: A reference volume is defined numerically that contains the light intensity pattern of one particle moving through its real image as shown in figure 4. The result is a cone along the optical axis. This synthetic reference volume is correlated with the volume determined in the previous paragraph. The result is a volume containing an accurate reconstruction of the seeding particles. With 1.5 Gbytes of memory, these calculations take typically 4 hours per reconstructed volume.
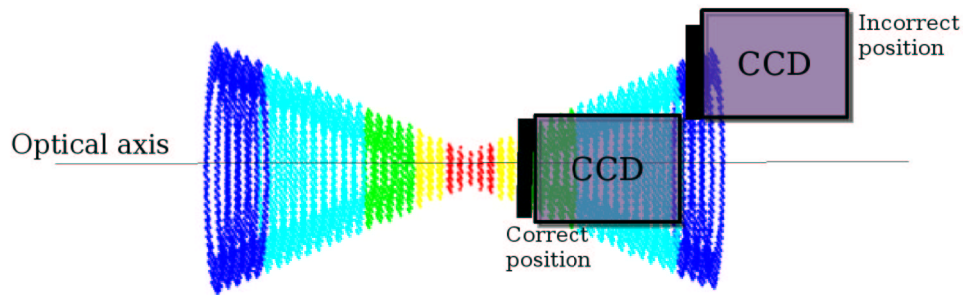

Figure 4. The 3-dimensional light intensity of a particle going through focus. The scale of the transverse axis does not correspond to the scale of the longitudinal axis.

3 Particle scattering

When designing a DHPIV setup it is very important to be aware of the light-scattering behavior of the seeding particles. For example, in section 4, the effect of various Fourier filters on the optical performance of the system is analyzed numerically. For a correct analysis, the light scattering pattern from a seeding particle must be known. Also, the light scattering pattern from a seeding particle must be known to reconstruct a hologram with an optimal signal-to-noise ratio. Further, as said in the introduction, ignoring the light scattering pattern can result in an effective NA of the setup that is lower than the nominal NA of the optical system. Finally, ignoring the anisotropy of the light scattering can also result in a diffraction limit that is not optimal. For these various reasons, experiments are performed to study the scattering behavior of the seeding particles.

Additionally, it is studied whether single-particle-scattering (and not multiple-particle-scattering) occurs. In the case of multiple particle scattering, some light that has scattered from a first particle becomes useless because it falls onto a secondary particle and does therefore not contribute to the signal of the hologram. This suppresses the signal-to-noise ratio. Also, light that falls onto a secondary particle does not have a clear phase throughout space, resulting in a relatively poor signal. For these reasons, single-particle-scattering is desirable for successful hologram recording, limiting the size and the density of the seeding particles in the measurement volume.

In this experiment, the power of the scattered light was measured as a function of two variables, the angle and the seeding density. The two following graphs (figures 5 left & right) show the same measurement results. The first graph clearly shows the decrease of light intensity with an increasing angle. If examined more closely, this graph also shows that for larger angles the light intensity increases with an increasing seeding density. For smaller angles however, the amount of scattered light reaches a maximum at a certain seeding density and then decreases if the seeding density is further increased. It is expected that this maximum represents the transition region between single-particle-scattering and multiple-particle-scattering. (Single-particle-scattering occurs at lower seeding density, while multiple particle scattering at higher seeding density.) The maximum is more clearly visible in the second graph.
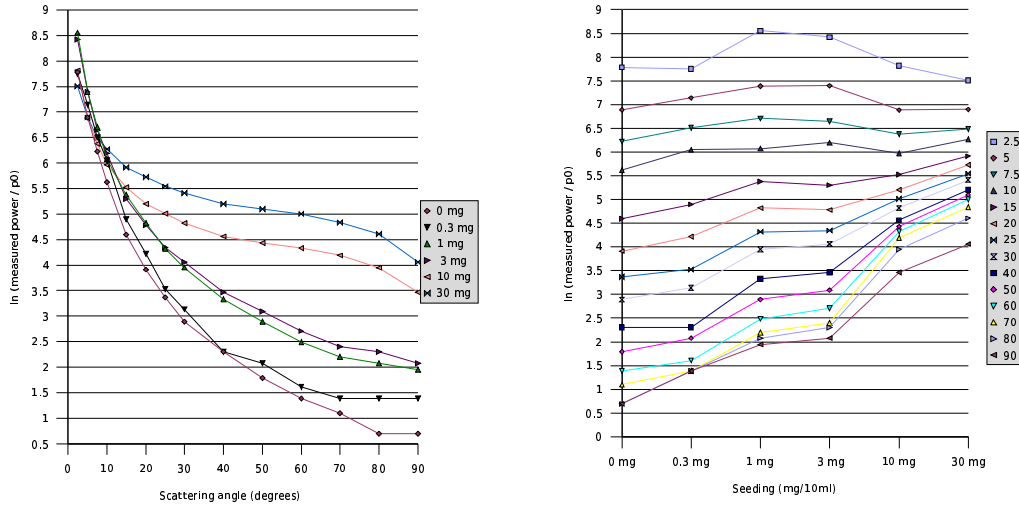
Figure 5. The measured light power as a function of the scattering angle and the seeding density. Both graphs show the same measurement data set. The value on both vertical axes is the 'ln' of the measured power divided by a reference power. This reference power, p0, is practically chosen 1 nW.

Because our imaging system is based on an in-line geometry, the light intensity pattern below 2.3 degrees is most relevant. However, the performed measurements only cover angles of 2.5 degrees and larger, because the presence of the bright unscattered beam prevented us from acquiring data at smaller angles. For this reason a fit was made to the 1mg/10ml data. The fit is then extrapolated towards smaller angles. It is expected that this extrapolation towards small values is, for 60 µm-particles, valid until 0.25 degrees, the estimated width of the main forward lobe. This angle can be derived in a short calculation where two light rays travel at an equal angle, 60 µm away from each other and their path length difference is one half of the wavelength. It is expected that at scattering angles larger than 0.25 degrees, the scattering intensity is a smooth continuous line. The data of 1mg/10ml is taken because this seeding is in the single-particle-scattering regime.

A fit in a log-log plot results in straight line, as shown in figure 6. The suggested formula of the fit is:

$$\text{Intensity (nW)} = A \cdot (\phi_{scatter})^{-B} \quad\quad\quad (4)$$

where A and B should be determined. A fit resulted in A = $4.01 \cdot 10^4$ nW and B = 1.95. Both the 1mg/10ml measurement data and the fit are shown in the figure 6. If the concept of particle-scattering is compared to light diffracting from a square-shaped aperture, it is expected that the light intensity pattern is a squared sinc as a function of a transverse spatial coordinate. Since the envelope of a squared sinc function is one divided by the spatial coordinate squared, B is expected to be close to 2. This supports the measurement result.

Formula (4), with the measured values for A and B can be used to study how the scattered light from a particle is affected by the presence of different Fourier filters in the DHPIV setup.
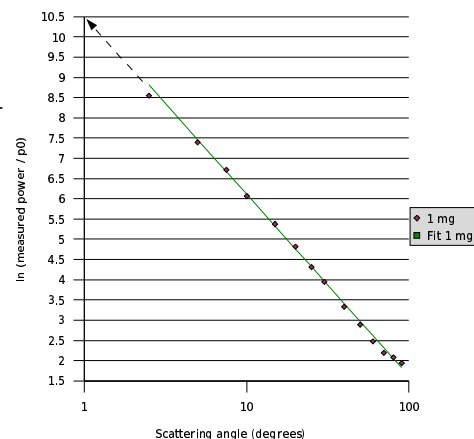

Figure 6. The 1mg/10ml measurement data and the fit are shown in this graph.

4 Optimizing Fourier Filtering.

The Fourier filter has a large influence on the NA, the depth of focus and the diffraction limit of the

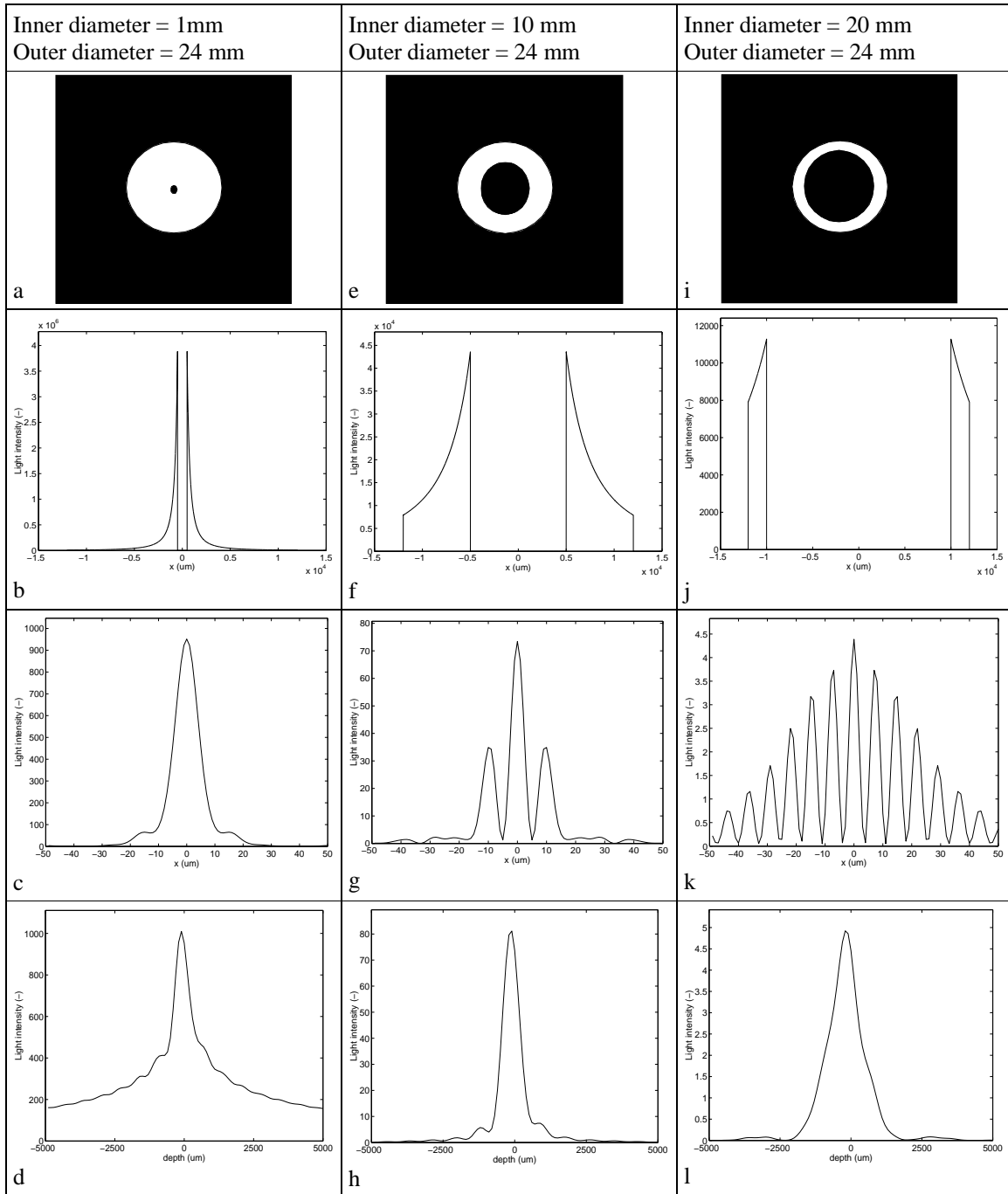| Inner diameter = 1mm Outer diameter = 24 mm	Inner diameter = 10 mm Outer diameter = 24 mm	Inner diameter = 20 mm Outer diameter = 24 mm

Figure 7. A numerical analysis. Figures a), e), i) show 3 Fourier filters that can be included in the setup. Black is opaque, white is transparent. The light intensity that passes through the filter as a function of the transverse coordinate, x, is shown in figure b), f), j). Figures c), g), k) show the light intensity of the real image as a function of the transverse coordinate x, representing the diffraction limit. Figures d), h), l) show the light intensity of the real image as a function of the longitudinal coordinate z, representing the depth of focus. The fringes in figure g and k are visible because the simulation uses an infinitely small pixel size. An optimized simulation, that accounts for the CCD pixel size, would show a smoother, bell-shaped curve.

system. This section shows that these optical parameters can be optimized by choosing an appropriate filter. Three different Fourier filters, consisting of a concentric opaque disc and a circular aperture are analyzed numerically and experimentally. The diameter of the opaque disc is chosen at 1 mm, 10 mm and

20 mm. The diameter of the circular aperture is constant, 24 mm.

The effect of these filters is numerically analyzed by placing one scattering particle on the optical axis, in the far left focal plane. The particle scatters anisotropically (as determined earlier), and the particle is regarded as a point-source. Due to the particle's strong anisotropic scattering, most of the light is concentrated near the central disc. For this reason, the central disc has a strong influence on the effective NA of the system. For the Fourier filter with the smallest diameter, the intensity profile in the Fourier plane is extended somewhat further towards zero degrees than the limit of 0.25 degrees described in the previous section. This may have a small effect on the results corresponding to the smallest filter.

As a result from this numerical analysis, the Fourier filter with the smallest diameter has a diffraction limit, or transverse resolution with an acceptable size. The depth of focus is relatively poor. Although in this numerical analysis the peak-position can be accurately determined, the large value of the side-tails could result in inaccurate z-position measurements if noise is present in the system.
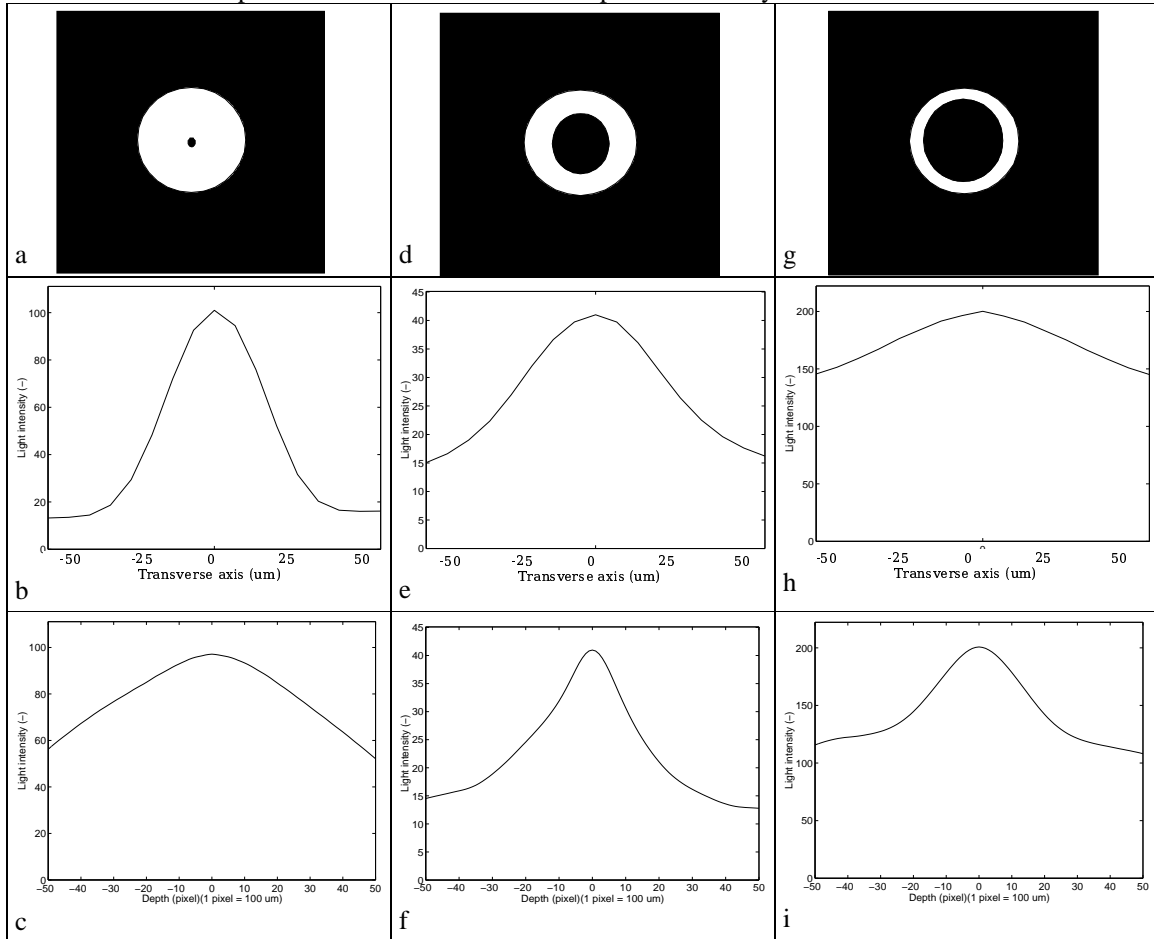

Figure 8. An experimental analysis. Figures a), d) & g) show the three applied Fourier filters, black is opaque, white is fully transmitting. Figures b), e) & h) show the light intensity near the reconstruction of seeding particles as a function of the transverse coordinate x, averaged for several particles. Figures c), f) & i) show the light intensity near the reconstructed seeding particle as a function of the longitudinal coordinate z, averaged over several particles. (The units on the intensity axis are random. Comparison between different graphs has no physical meaning.)

In the numerical analysis, the second Fourier filter shows a larger diffraction limit, but with a value smaller than the particle diameter. The profile of the depth resolution has improved greatly. The light intensity, however, has decreased by a factor 10.

In the numerical analysis, the third Fourier filter shows an unacceptably large diffraction limit. Because the

diffraction limit is related to the depth profile, it also results in a poorer depth of focus. Additionally, the light intensity has been reduced by a factor 200 when compared to the first filter.

In the experimental analysis, the graphs of the transverse intensity profile clearly illustrate an increasing diffraction limit for a narrower Fourier filter. This result matches the numerical expectation in figure 7. The third row verifies the numerical expectation that the intermediate 10mm-Fourier filter gives the best depth of focus.

The numerical and experimental results both indicate that the 10mm-Fourier filter shows an optimal performance.

It is also possible to construct more complicated filters that compensate for the anisotropic scattering (where the transmission is a smooth function of x and y), but preliminary calculations show that such filters barely perform better than the simpler filters already described.

5 Measurement results

Because the whole success of a DHPIV set-up depends on the accuracy with which a particle's position can repeatedly be determined, an experiment is performed to determine this accuracy: Seeding particles in resin are placed in the location of the measurement volume. The particles are accurately moved along the optical axis with steps of 1 millimetre. During each step, a hologram is recorded, and the particle's 3-dimensional image reconstructed.

The picture below shows five slices through the five 3-dimensional images. Each slice corresponds to a different particle position along the optical axis. The particle's position is expected to shift 1 millimetre between each slice, this expectation is illustrated by the white diagonal line.
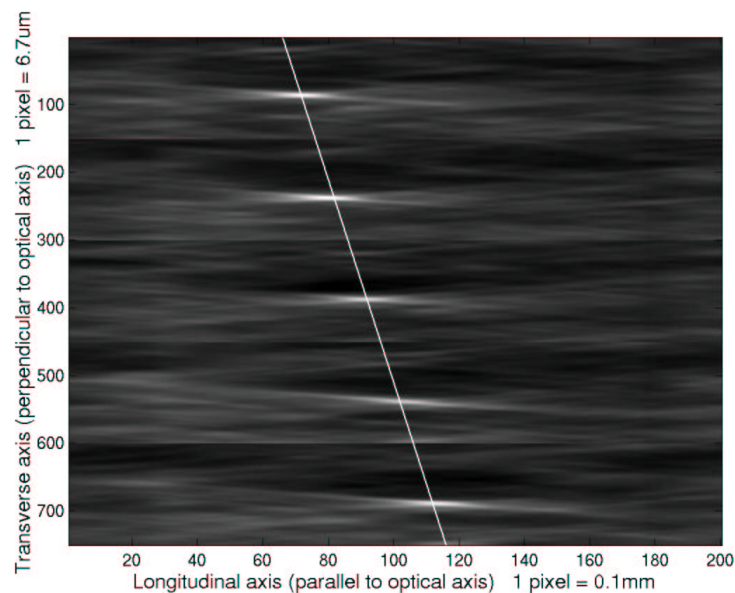

Figure 9. Five slices through five reconstruction volumes showing a seeding particle at five different locations along the optical axis. The grey shade represents the light intensity. The particle is expected to move 1 millimetre between each step, an expectation illustrated by the white line.

To analyse the above step sizes, a 3-D parabolic fit is made on the 7 points nearest to the maximum light intensity. The maximum of this 3-D parabola is determined. The location difference between two maxima should result in five longitudinal shifts of 0 μm, in four shifts of 1000 μm, three shifts of 2000 μm, two shifts of 3000 μm and one shift of 4000 μm. The results are shown in the graph below.
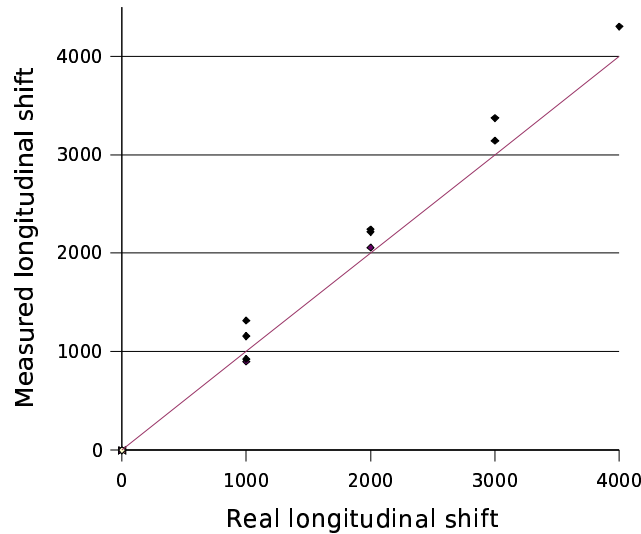
Figure 10. The measurement results of the particle shifts. The line represents the real longitudinal shift. The points represent the measured longitudinal shifts.

The longitudinal component of the shift is on average larger than the expectation. This effect is probably caused by a small magnification by the two lenses of the Fourier filter.

The parabolic fit also results transverse components of the shifts. These transverse components were reconstructed with an inaccuracy of a few microns.

6 Conclusions & Future work

This paper shows that the effective NA, the depth of focus and the diffraction limit of a DHPIV system can be optimized by applying appropriate Fourier filtering.

First, the experimental setup and the method for the numerical three-dimensional reconstruction are described. A cone-shaped reference volume is defined and successfully applied to optimize the signal-to-noise ratio of the reconstruction.

Further, in section 3, the relevance of the particle scattering pattern was explained and the pattern is determined by measurements. For the used particles, the light intensity depends on the scattering angle via the power-law given in formula (4). This power-law indicates that the forward scattered light is much stronger than the sideward scattered light. Therefore, to reach the highest hologram exposure, the near-forward-scattered light is used to record a hologram.

An optimal Fourier filter is designed and applied to the set-up, as described in section 4. It is shown that the intermediate Fourier filter, with an inner diameter of 10 mm shows an improved optical performance. Figure 1 confirms that the depth of focus is optimal for the 10-mm-Fourier filter and that there is no significant increase of the diffraction limit.

With this knowledge, we expect that there is possibly room for NA-improvement in other recently published DHPIV systems. Some publications have described experimental setups with small high-pass filters [1][2], and some with no Fourier filtering at all [3][5][9].

Although roughly 10 times less light reaches the CCD camera with the 10-mm-configuration compared to the 1-mm-configuration, successful recordings can still be made. During the exposure time of 500 μsec, the continuous wave 150 mW laser delivers 75 μJ to the system. A pulsed laser could easily deliver 75 mJ per pulse. Hence, the reduction in hologram exposure due to the improved Fourier filter can easily be

compensated by using an appropriate laser.

As shown in section 5, the accuracy with which a particle position can be reconstructed along a transverse axis is in the order of a few microns. The accuracy with which a particle position can be reconstructed along the longitudinal axis is a few hundred microns. These inaccuracies are close to the reported inaccuracies of optical holographic PIV systems using high-resolution films. The transverse field of view in DHPIV however, remains limited with the current CCD chip size.

Finally, future work includes the optimization of the seeding particle size. The current particles in the setup have a diameter of 60 μm. It is expected that, while the particle size is larger than the diffraction limit of the system, roughly 30 μm, the transverse size and longitudinal size (= depth of focus) of the particle image both scale proportional to the particle size. In order to further reduce the depth of focus, particles with a diameter of 30 μm will be implemented in the future.

7 Acknowledgements

8 References

[1] Sheng J., Malkiel E., Katz J., Single beam two-views holographic particle image velocimetry, Appl. Optics, 42, 235-250, 2003.
[2] Zhang J.,Tao B., Katz J., Turbulent flow measurement in a square duct with hybrid holographic PIV, Exp. Fluids, 23, 373-381, 1997
[3] E. Malkiel, J. Sheng, J. Katz, J.R. Strickler, 'The 3-dimensional flow field generated by a feeding calanoid copepod measured using digital holography.', The Journal of Experimental Biology 206, 3657-3666 (2003)
[4] Kreis, Jüptner, Fringe '97, 353-363, (Springer 1997)
[5] G. Pan and H. Meng, "Digital Holography of Particle Fields: Reconstruction using Complex Amplitude", Applied Optics, 42(5) 827-833 (2003).
[6] M. Raffel, C. Wilert, J.Kompenhans, "Particle Image Velocimetry, A Practical Guide", Springer, 1998
[7] K.D. Hinsch, 'Advanced Optical Techniques', Course Notes, Application of PIV, Goettingen 2004
[8] Liu F., Hussain F., Holographic Particle Velocimeter Using Forward Scattering with Filtering, Optics Letters, Vol.23 No.2, 1998
[9] K. Ikeda, K. Okamoto, S. Murata, 'Development of Dynamic Digital Holographic Particle Velocimetry.' 5th International Symposium on Particle Image Velocimetry, PIV Paper 3103, Busan Korea, September 22-24, '03
[10] J.W. Goodman, Introduction to Fourier Optics, McGraw-Hill, 1996